

## Towards a fully 3D MHD plasma-structures model: Coupling JOREK and CARIDDI

N. Isernia<sup>1</sup>, N. Schwarz<sup>2</sup>, F. J. Artola<sup>3</sup>, S. Ventre<sup>4</sup>, G. Rubinacci<sup>1</sup>, M. Hoelzl<sup>2</sup>, F. Villone<sup>1</sup>

<sup>1</sup> Consorzio CREATE, DIETI, Università degli Studi di Napoli Federico II, IT

<sup>2</sup> Max Planck Institute for Plasma Physics, Garching, DE

<sup>3</sup> ITER Organization, Route de Vinon sur Verdon, 13067 St Paul Lez Durance Cedex, FR

<sup>4</sup> Consorzio CREATE, DIEI, Università degli Studi di Cassino e del Lazio Meridionale, IT

### Introduction

Passive conductors represent an essential element of all existing tokamak devices, since eddy currents slow down Alfvénic instabilities to the electromagnetic time scale [1]. Shared currents between plasma and conductors, defined as *halo currents*, have also been routinely observed during *disruptions* of experiments. The 3D features of conducting structures affect plasma vertical stability properties [2] and can be responsible for mode locking or braking. Consequently, realistic macroscopic simulations of tokamak plasma dynamics require to capture the mutual interaction of a 3D plasma model with an accurate 3D model of conducting structures. However, complete 3D extended-MHD models generally use a simplified description of passive conductors (*e.g.* 2D or thin), and detailed 3D models of conductors are self-consistently coupled only to simplified MHD plasma models [3].

Here we illustrate a coupling scheme, based on the Virtual Casing principle, for the self-consistent integration of the 3D non-linear extended-MHD model of the JOREK code [4] with the fully 3D volumetric model of conducting structures implemented in CARIDDI [5]. This is the same scheme earlier adopted for the JOREK-STARWALL coupling [6].

### Coupling Scheme

The Magneto-Hydro-Dynamic models implemented in JOREK use the total magnetic vector potential  $\mathbf{A}$  as primary variable. The resulting differential formulation requires to prescribe the tangential magnetic field at the boundary of the computational domain  $\mathbf{B}_{\text{tan}} = \mathbf{B} \times \hat{\mathbf{n}}$ .

The tangential component of the magnetic vector potential at the MHD computational boundary  $\mathbf{A}_{\text{tan}} = \mathbf{A} \times \hat{\mathbf{n}}$  and the current density  $\mathbf{j}$  in external conductors are sufficient to determine the plasma magnetic field in the outer domain. Accordingly, we use this information to determine the equivalent surface current to the plasma, placed at the JOREK boundary. As long as there

are no currents crossing the boundary, we can impose Biot-Savart law in weak form on a set of basis functions which is divergence-free at the MHD domain boundary. We discretize the JOREK boundary with a layer of infinitesimally thin CARIDDI hexahedral elements, setting up a Galerkin method:

$$\int_{V_{eq}} \mathbf{w}_j \cdot (\mathbf{A} - \mathbf{A}_w) dV = \sum_{k=1}^{N_{eq}} I_{eq,k} \frac{\mu_0}{4\pi} \int_{V_{eq}} \int_{V'_{eq}} \frac{\mathbf{w}_k(\mathbf{r}') \cdot \mathbf{w}_j(\mathbf{r})}{|\mathbf{r} - \mathbf{r}'|} dV' dV \quad (1)$$

Here the test functions  $\mathbf{w}_k$  are tangential to the boundary and divergence-free therein. In particular, the overall magnetic vector potential  $\mathbf{A}$  is expressed in terms of JOREK basis functions, while the  $\mathbf{A}_w$  is expressed via Biot-Savart law, again in terms of CARIDDI basis functions. In compact matrix notation, the CARIDDI equivalent currents to the plasma are related to the overall magnetic vector potential and to the external currents via the relation

$$\underline{\underline{H}} \underline{\underline{A}} - \underline{\underline{M}}_{eq,w} \underline{\underline{I}}_w = \underline{\underline{L}}_{eq} \underline{\underline{I}}_{eq} \quad (2)$$

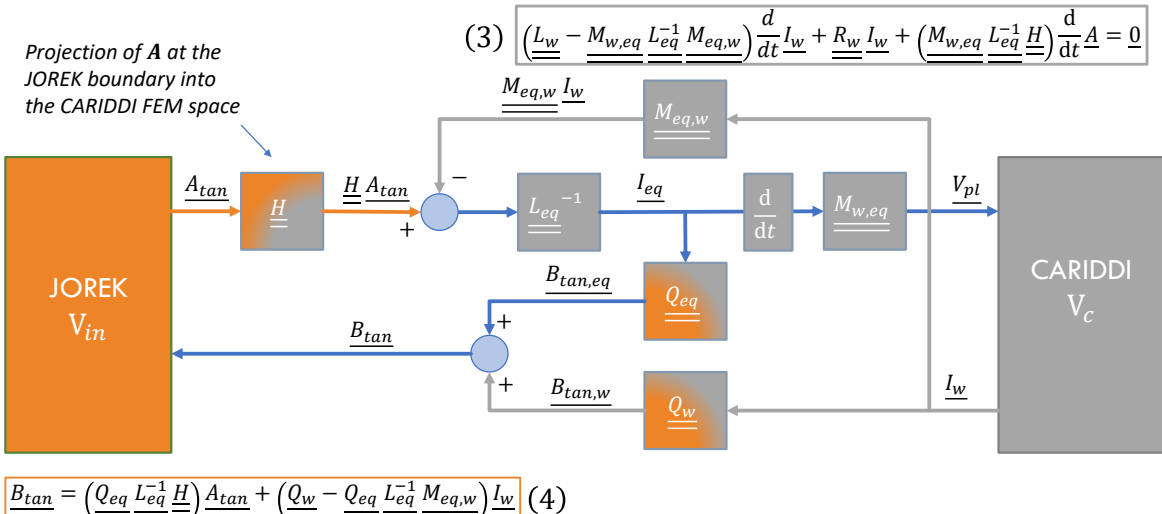


Figure 1: Schematic of the coupling approach adopted, based on the Virtual Casing Principle.

The evolution equation (3) for the external currents is integrated by JOREK, exploiting the generalized eigenvectors and eigenvalues of the problem. The *modified* inductance matrix in brackets, physically corresponds to the inductance matrix of external structures in presence of an ideal wall at the JOREK boundary. The matrices  $\underline{\underline{Q}}_w$  and  $\underline{\underline{Q}}_{eq}$  in equation (4) provide the magnetic field at the JOREK boundary due to external and equivalent currents respectively. As before, the magnetic field matrix  $\left( \underline{\underline{Q}}_w - \underline{\underline{Q}}_{eq} \underline{\underline{L}}_{eq}^{-1} \underline{\underline{M}}_{eq,w} \right)$  provides the magnetic field due to external currents in presence of an ideal wall at the JOREK boundary. The remainder magnetic field due to actual fluxes at the JOREK boundary is provided via the matrix  $\left( \underline{\underline{Q}}_{eq} \underline{\underline{L}}_{eq}^{-1} \underline{\underline{H}} \right)$ .

## Preliminary Tests

The matrices required by JOREK reduced MHD models for evolving the  $B_{tan}$  boundary condition are now computed by new routines implemented within the CARIDDI code. A simple axisymmetric MHD equilibrium test was used to validate the efficacy of the implementation, scanning with the toroidal resolution used to discretize the JOREK boundary. The overall poloidal flux at the JOREK boundary was provided by a JOREK-STARWALL equilibrium, and the set of active coil currents was implemented using standard hexahedral CARIDDI elements. A summary of the data used for the axisymmetric tests is given in Figure 2, together with the overall tangential magnetic field computed at the JOREK boundary.

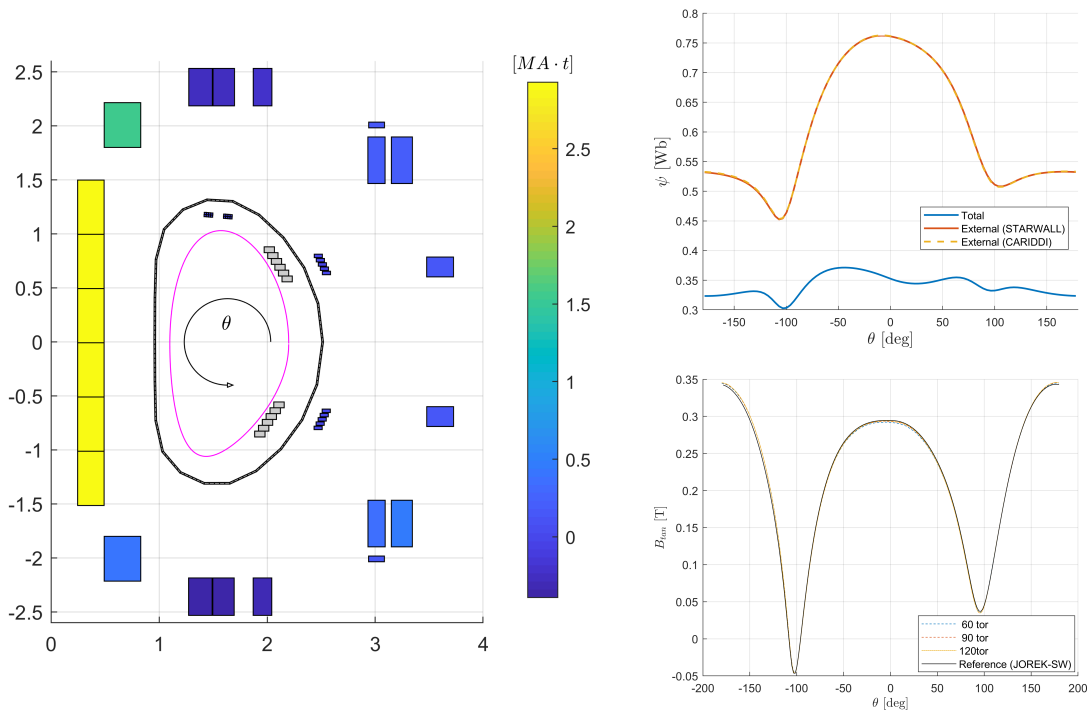


Figure 2: (a) Reference geometry for JOREK boundary, passive structures and coil currents; (b) Poloidal flux at the JOREK boundary; (c) Comparison of overall magnetic field for different toroidal discretizations of the JOREK boundary.

The match with the reference magnetic field improves with the toroidal resolution, as expected. The adequacy of the computed matrices in providing the boundary conditions to JOREK is demonstrated by two simple numerical experiments. First, we compute a JOREK free-boundary equilibrium using the magnetic field matrices provided by CARIDDI. The small mismatch between the results obtained via CARIDDI and STARWALL matrices should be attributed to the different discretization of active coils and JOREK boundary. Second, the free-evolution of this vertically unstable plasma is qualitatively compared with a JOREK-STARWALL simulation. The slightly different evolution of the magnetic axis is probably determined by the different models of the Passive Plates implemented in CARIDDI and STARWALL.

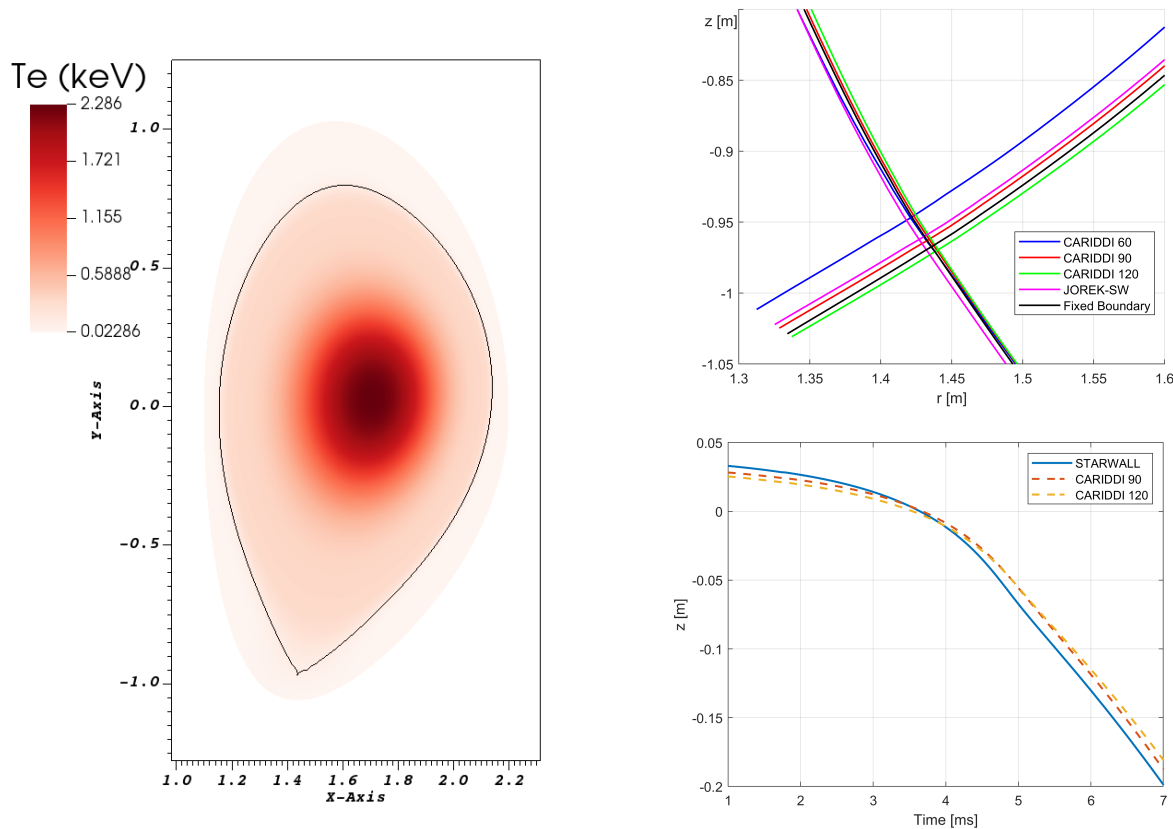


Figure 3: (a) Free-boundary equilibrium with JOREK-CARIDDI (120 toroidal elements); (b) Comparison of free-boundary separatrix as computed with different discretizations. (c) Free-evolution, magnetic axis vertical position.

## Perspectives

The coupling of JOREK with CARIDDI will offer the first self-consistent numerical tool to simulate the interaction of 3D tokamak plasmas with fully volumetric 3D conductors nearby. First simulations with realistic ASDEX-U conductors geometry are planned soon within this framework. For the moment no-wall tests indicate accurate prediction of tearing mode growth-rate, supporting further the efficacy of our vacuum response matrix. On the longer term, we plan to extend our approach to the simulation of halo currents. This will require to recover the information discarded projecting  $\mathbf{A}_{tan}$  onto divergence-free basis in the JOREK boundary.

This work has been carried out within the framework of the EUROfusion Consortium, funded by the European Union via the Euratom Research and Training Programme (Grant Agreement No 101052200 — EUROfusion). Views and opinions expressed are however those of the author(s) only and do not necessarily reflect those of the European Union or the European Commission. Neither the European Union nor the European Commission can be held responsible for them.

## References

- [1] E. A. Lazarus et al., Nuclear Fusion **20**, 111 (1990)
- [2] R. Albanese et al., Nuclear Fusion **44**, 999 (2004)
- [3] F. Villone et al., Plasma Physics and Controlled Fusion **55**, 095008 (2013)
- [4] M. Hoelzl et al., Nuclear Fusion **61**, 065001 (2021)
- [5] R. Albanese and G. Rubinacci, IEE Proceedings A **135**, 457 (1988)
- [6] M. Hoelzl et al., Journal of Physics: Conference Series **401**, 012010 (2012)